

# Magnetic anisotropy of vicinal (001) fcc Co films: Role of crystal splitting and structure relaxation in the step-decoration effect

M. Cinal\*

*Institute of Physical Chemistry of the Polish Academy of Sciences, ul. Kasprzaka 44/52, 01-224 Warszawa, Poland*A. Umerski<sup>†</sup>*Department of Applied Mathematics, Open University, Milton Keynes MK7 6AA, United Kingdom*

(Received 12 December 2005; revised manuscript received 11 April 2006; published 18 May 2006)

The uniaxial in-plane magnetic anisotropy (UIP-MA) constant is calculated for a single step on the (001) surface of fcc Co(*N*) films. The calculations are done for both an undecorated step and the step decorated with one or more, up to seven, Cu wires. Our objective is to explain the mechanisms by which the decoration decreases the UIP-MA constant, which is the effect observed experimentally for ultrathin Co films deposited on vicinal (001) Cu surfaces and can lead to reorientation of magnetization within the film plane. Theoretical calculations performed with a realistic tight-binding model show that the step decoration changes the UIP-MA constant significantly only if the splitting between the on-site energies of various *d*-orbitals is included for atoms located near the step edge. The local relaxation of atomic structure around the step is also shown to have a significant effect on the shift of the UIP-MA constant. The influence of these two relevant factors is analyzed further by examining individual contributions to the UIP-MA constant from atoms around the step. The magnitude of the obtained UIP-MA shift agrees well with experimental data. It is also found that an additional shift due to possible charge transfer between Cu and Co atoms is very small.

DOI: [10.1103/PhysRevB.73.184423](https://doi.org/10.1103/PhysRevB.73.184423)

PACS number(s): 75.30.Gw, 75.70.Cn, 75.70.Ak

## I. INTRODUCTION

The magnetic anisotropy (MA), determined by the dependence of energy on the orientation of magnetization, is one of the basic properties of magnetic systems. A nonzero MA energy arises due to two different physical effects: long-range magnetic dipole-dipole interaction and spin-orbit (SO) coupling. The latter interaction couples the spin of an electron to the local electric field as the electron travels through the system which makes the interaction sensitive to the local atomic structure. This leads to the magnetocrystalline (MCA) component of the MA energy. As the symmetry is reduced in nanoscopic structures, the MCA energy (per atom) becomes larger, normally by two orders of magnitude, than in bulk cubic crystals.<sup>1,2</sup> An example of such low symmetry structures is a ferromagnetic ultrathin film deposited on a vicinal surface which consists of monoatomic steps separated by flat terraces.<sup>7,8</sup> Vicinal surfaces can be obtained by slightly mis-cutting low-index [e.g., (001)] surfaces of substrate crystal.

In the present paper, we study theoretically MA of fcc Co films placed on a vicinal (001) Cu surface with step edges running along the direction  $[1\bar{1}0]$ . In such systems, the magnetization  $\mathbf{M}$  lies within the Co film plane due to the negative sign of the out-of-plane MA constant  $K_2$  which determines the energy dependence  $K_2 \sin^2 \theta$  on the magnetization polar angle  $\theta$ ; cf. Ref. 3. With  $\mathbf{M}$  lying in-plane (i.e., for  $\theta = \pi/2$ ), the system energy depends on the azimuthal angle  $\phi$  which  $\mathbf{M}$  makes with the  $[1\bar{1}0]$  axis,

$$E(\phi) = K_1/4 \sin^2(2\phi) + K_u \sin^2 \phi - MH \cos(\phi - \phi_H). \quad (1)$$

Here, the first term on the right-hand side is due to biaxial (fourfold) MA which arises because the directions  $[110]$  and

$[100]$  are nonequivalent in systems with cubic crystal structure. The cubic MA constant  $K_1$  is positive for fcc Co/Cu(001) films.<sup>4</sup> Thus, in flat Co/Cu(001) films the magnetization lies along one of the two equivalent directions:  $[110]$  or  $[1\bar{1}0]$ , the easy axes, while the directions  $[100]$ ,  $[010]$  are hard axes. The existence of steps in vicinal Co/Cu(001) films introduces an additional, uniaxial (two-fold), magnetic anisotropy within the film plane. The directions  $[110]$  and  $[1\bar{1}0]$  cease to be equivalent: one of them remains the easy axis, the other becomes the intermediate axis.<sup>5,6</sup> The sign of the uniaxial in-plane MA (UIP-MA) constant  $K_u$ , equal to

$$K_u = E(\phi = \pi/2) - E(\phi = 0), \quad (2)$$

at  $H=0$ , determines the easy direction of magnetization:  $\mathbf{M}$  is parallel (perpendicular) to the step edges when  $K_u$  is positive (negative).

The expression (1) includes, optionally, an external magnetic field  $\mathbf{H}$  which is assumed to lie within the film plane at the azimuthal angle  $\phi_H$  to the  $[1\bar{1}0]$  axis. Experimentally, by applying the field  $\mathbf{H}$  perpendicularly to the easy axis, one can measure the so-called shift field  $H_s$  and determine the UIP-MA constant as

$$K_u = H_s M_s; \quad (3)$$

here  $M_s$  is the saturation magnetization.<sup>5</sup> This relation holds as long as  $K_u$  is much smaller than  $K_1$  which is true for vicinal Co/Cu(001) films.<sup>5</sup>

The magnetic anisotropy of thin ferromagnetic films deposited on nonmagnetic vicinal surfaces has been the subject of many experimental papers. Apart from Co/Cu(001)

systems,<sup>5–7,9–13</sup> the reported work also concerned Fe films on vicinal Ag, Au, W, Pd, Cr (001) substrates<sup>14–20</sup> and vicinal Ni/Cu(001) systems.<sup>21</sup> Related experimental measurements of UIP-MA have been performed for Co/Cu(110) ultrathin films<sup>22–24</sup> and also for Co films obtained by depositing Co atoms at an oblique angle on a flat (001) Cu surface which leads to some structural anisotropy.<sup>25</sup> In the experiments on MA in vicinal films, it was investigated how the shift field  $H_s$  depends on the ferromagnetic film thickness, the miscut angle  $\alpha$  and the miscut direction.<sup>19</sup> These dependencies were found to be determined by the kind of the deposited film, its lattice type, the choice of substrate, and, in consequence, also by the strain present in the film. For Co/Cu(001) systems, the UIP-MA constant  $K_u$  has been found to depend linearly on the miscut angle  $\alpha$  which implies that  $K_u$  is proportional to the step density; cf. Eq. (4) below. The experimental dependence on the Co film thickness  $d$  is more complicated: the usual breakdown,<sup>26</sup>  $K_u = K_u^v + K_u^s/d$  into the volume and surface terms is not generally valid, presumably, due to the anisotropic relaxation of the biaxial strain present in Co/Cu systems.<sup>12</sup>

Covering a vicinal ferromagnetic film with nonmagnetic adsorbates, like Cu, Ag, O or CO, usually has a large effect on UIP-MA.<sup>7,9,24</sup> In particular, it has been found experimentally that even submonolayer amount of Cu deposited on a vicinal Co film can decrease  $K_u$  so significantly that, in some cases,  $K_u$  becomes negative and the magnetization direction switches to perpendicular to the steps.<sup>5–7,9–12</sup> This effect is usually explained by change in local MCA due to Co-Cu orbital hybridization at Co step edges after they are decorated with Cu atoms.<sup>27</sup> Such qualitative explanation seems plausible, however it still requires further investigation since few, and only partly relevant, theoretical calculations have been done so far. In Ref. 28, the energy of a single step on a (001) fcc Co film with noncollinear magnetic structure was calculated within an *ab initio* model without SO coupling included. However, no values for the UIP-MA constants nor definite conclusions about the magnetization reorientation were given there. The relativistic full-potential linear-augmented-plane-wave calculations,<sup>29</sup> performed for a planar network of parallel Co wires separated with empty wires (i.e., a striped monolayer), have shown that magnetization changes its orientation upon filling the empty wires with Cu. However, this structure seems too simplified to extend the obtained results to the case of Co vicinal films. In Ref. 30, more realistic systems, i.e., unsupported stepped Co and Fe monolayers were considered using a tight-binding (TB) model, but the effect of step decoration was not studied. The present authors reported<sup>31</sup> a TB calculation for a monoatomic step on a 5 monolayer (ML) (001) fcc Co film. It was found that the MCA contribution  $K_u^{\text{MCA}}$  to the UIP-MA constant  $K_u$  was only slightly shifted after step decoration and the shift was much smaller than experimental values (cf. Sec. III). With the same TB model, shifts of  $K_u^{\text{MCA}}$  by similar or smaller magnitude were found for steps on Co films with thicknesses other than 5 ML (in the range 2 up to 10 ML).

The present theoretical study focuses on explaining the mechanisms by which decoration of Co steps with Cu atoms changes UIP-MA in vicinal Co/Cu(001) systems. We calculate  $K_u^{\text{MCA}}$  for stepped Co films using an improved TB model.

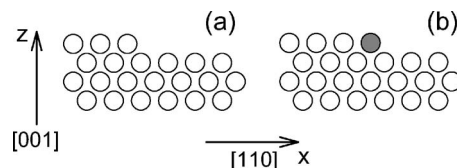


FIG. 1. Geometric structure of (001) fcc  $\text{Co}(N/N-1)$  step: (a) undecorated, (b) decorated with one Cu atomic wire (shaded circle).

This model includes crystal field splittings (CFS) introduced into the on-site energies of  $d$  orbitals on every atom in the system. Similar, though simplified, CFS have previously been included and shown to play a crucial role in calculations of the out-of-plane MA constant of flat films and multilayers.<sup>32–37</sup> Here, we also investigate how the UIP-MA constant is modified by the relaxation in the Co film structure around the step. In addition, a potentially significant effect of the charge transfer (CT) between Cu and Co atoms in the decorated steps is studied. We do not include the contribution to UIP-MA coming from the dipole-dipole interaction because it remains almost unchanged when the Co steps are decorated with nonmagnetic atoms (cf. Sec. III and Ref. 38).

## II. MODEL

### A. Geometry: Structure relaxation

In experiment, cobalt films deposited with molecular beam epitaxy grow pseudomorphically on the vicinal (001) Cu surface for film thicknesses larger than 2 monolayers (ML) and less than 10–15 ML.<sup>12</sup> Thus, the Co film surface replicates the underlying stepped substrate surface quite well in this thickness regime. When a submonolayer amount of copper is next deposited on such vicinal films, Cu atoms decorate the Co step edges as has been shown by scanning-tunneling-microscope measurements.<sup>27</sup>

The miscut angle  $\alpha$  determines the terrace width and consequently the number  $N_{\text{rows}}$  of atomic rows (lying parallel to  $[1\bar{1}0]$ ) on each terrace,<sup>13</sup>

$$N_{\text{rows}} = \frac{1}{\sqrt{2} \tan \alpha}. \quad (4)$$

The steps on vicinal surfaces are normally well separated. Indeed,  $N_{\text{rows}}$  is equal to approximately 400, 25, 12 atomic rows for the vicinal Co/Cu(001) systems with small miscut angles  $\alpha=0.1^\circ$ ,  $1.6^\circ$ ,  $3.4^\circ$ , respectively, which were studied experimentally in Refs. 5–7,9–12. Therefore, as the decoration of a given step is expected to change MCA only locally, we restrict our theoretical model to a single monoatomic step on Co (001) fcc film. For further simplicity, we assume that the step is present only on the upper film surface and the bottom surface is flat so the system, hereafter called  $\text{Co}(N/N-1)$  step, is actually built of two joined semi-infinite slabs with thicknesses of  $N$  and  $N-1$  monolayers, correspondingly [Fig. 1(a)]. For the decorated systems, there are one or more Cu wires attached to the step edge on the upper surface on the Co film [Fig. 1(b)]. For later reference, we assume that the axes  $x$ ,  $y$ ,  $z$  are along the directions  $[110]$ ,

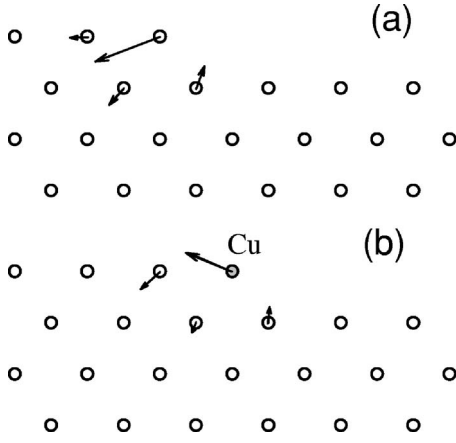


FIG. 2. Relative displacements (arrows) of the atomic positions in the biaxially strained lattice around the edge of the (001) fcc Co(4/3) step: (a) undecorated, (b) decorated with one Cu wire. The arrows are 30 times longer than the actual displacements relative to the lattice.

$[1\bar{1}0]$ , and  $[001]$ , correspondingly, and the step-edge Co wire is located at the position  $x=0$ ,  $z=0$ .

Owing to the 1.8% mismatch between the lattice constants of cobalt and copper, the cobalt film is subject to biaxial strain. This leads to tetragonal distortion of the Co film lattice: the in-plane distances between Co atoms are expanded, to match the Cu lattice constant, while the distances between Co planes become compressed in comparison to bulk fcc Co lattice. In the present work, we consider Co( $N/N-1$ ) steps of thicknesses  $N \leq 10$  which have either (i) perfect or (ii) tetragonally distorted fcc lattice. In the latter case, we allow for additional relaxation of the atomic positions in the vicinity of the step. The relaxed atomic positions  $\mathbf{R}_i$  are obtained by minimizing the system energy

$$E(\mathbf{R}_1, \mathbf{R}_2, \dots) = E_B(\mathbf{R}_1, \mathbf{R}_2, \dots) + \frac{1}{2} \sum_{ij, i \neq j} V_P(\mathbf{R}_i - \mathbf{R}_j). \quad (5)$$

It includes the band energy  $E_B$  and the pair potentials  $V_P$  which are given by the analytical formulas with parameters fitted<sup>39</sup> to reproduce various elastic properties either known from experiment for Cu or found with first-principle methods for Co and Co/Cu systems. This semiempirical model, based on the second moment tight-binding approximation, was previously used to find strain relief and shape evolution for a Co island on Cu surface.<sup>40</sup> Here, we use the model to calculate the displacements of atomic positions around the step edge. These displacements (magnified by a factor of 30) are depicted for the Co(4/3) step in Fig. 2; very similar shifts are found for Co(8/7) step. They are shown relative to the biaxially strained slabs, Co( $N$ ) and Co( $N-1$ ), for which the interlayer spacings are also obtained with Eq. (5).

### B. Tight-binding model: Crystal field splittings

The electronic structure is described with an extended TB Hamiltonian,

$$H_{\text{TB}} = \sum_i \sum_{\mu\nu} \sum_{\sigma} V_{i\mu\nu}^{\sigma} c_{i\sigma\mu}^{\dagger} c_{i\sigma\nu} + \sum'_{ij} \sum_{\mu\nu} \sum_{\sigma} T_{i\mu;j\nu}^{\sigma} c_{i\sigma\mu}^{\dagger} c_{j\sigma\nu} + H_{\text{SO}}(\theta, \phi). \quad (6)$$

Here,  $\mu$ ,  $\nu$  denote any of nine orbitals, of  $s$ ,  $p$ , or  $d$  symmetry, located on every atom (Co or Cu), labeled with index  $i$  or  $j$ ;  $\sigma$  is spin and  $c^{\dagger}$ ,  $c$  are creation and annihilation operators, respectively. The Hamiltonian depends on the magnetization direction  $(\theta, \phi)$  through the SO interaction

$$H_{\text{SO}}(\theta, \phi) = \sum_i \sum_{\mu\nu} \sum_{\sigma\sigma'} \xi_i \langle \mu\sigma | \mathbf{L} \cdot \mathbf{S} | \nu\sigma' \rangle c_{i\mu\sigma}^{\dagger} c_{i\nu\sigma'}, \quad (7)$$

where the elements  $\langle \mu\sigma | \mathbf{L} \cdot \mathbf{S} | \nu\sigma' \rangle$  are the known analytical functions of  $\theta$ ,  $\phi$  (cf. Ref. 41). We assume the SO constant  $\xi_i = 0.085$  eV for Co atoms,<sup>34–36</sup> and  $\xi_i = 0.10$  eV for Cu atoms.<sup>42–44</sup>

The elements  $T_{i\mu;j\nu}^{\sigma}$  describing electron hopping are calculated with the Slater-Koster (SK) formulas;<sup>45</sup> the sum over  $j$  in Eq. (6) includes the first and second nearest neighbors for every atom  $i$ . We assume the values of two-center hopping integrals found for paramagnetic fcc bulk Co in Ref. 46 by fitting to the *ab initio* band structure. When strain and structure relaxation are present, the hopping elements  $T_{i\mu;j\nu}^{\sigma}$  are obtained by using the canonical scaling law:  $|\mathbf{R}_i - \mathbf{R}_j|^{-(l+l'+1)}$ ; here  $l$  and  $l'$  are the orbital quantum numbers for orbitals  $\mu$  and  $\nu$  centered on atoms  $i$  and  $j$  which are located at the positions  $\mathbf{R}_i$  and  $\mathbf{R}_j$ , accordingly; cf. Ref. 47. The hopping two-center integrals between Co and Cu atoms are approximated by the geometric means of the corresponding Co and Cu integrals.

The generalized on-site energies  $V_{i\mu\nu}^{\sigma}$  (also known as on-site potentials)

$$V_{i\mu\nu}^{\sigma} = U_{i\mu\nu;\sigma} \delta_{\mu\nu} + V_{i\mu\nu}^{\text{CFS}} \quad (8)$$

consist of two terms. The first one, diagonal in  $\mu$ ,  $\nu$ , has a common value  $U_{i\mu\nu;\sigma}$  for all orbitals  $\mu$  of given angular symmetry,  $s$ ,  $p$  or  $d$  (corresponding to  $l=0$ , 1 or 2). The other term describes CFS, i.e., possibly different values of  $V_{i\mu\mu}^{\sigma}$  for various orbitals  $\mu$  with the same  $l$ ; in addition, nonzero elements  $V_{i\mu\nu}^{\text{CFS}}$  with  $\mu \neq \nu$  may exist. The CFS arise because various orbitals centered on a given atom  $i$  are oriented differently with respect to neighboring atoms which contribute to the electron potential  $V^{\sigma}(\mathbf{r})$  on and around the atom  $i$ . The TB parametrizations for bulk cubic crystals, like that in Ref. 46, include CFS, as the splitting between the on-site energies of  $t_{2g}$  and  $e_g$  orbitals. However, CFS are often neglected in TB models for systems with lower symmetry like surfaces (cf., e.g., Refs. 30 and 48) even though the corresponding CFS are larger than in bulk.<sup>49</sup> The splitting between the on-site energies of  $d$  orbitals oriented out-of-plane and those lying in-plane, located on atoms at the film surface (or at an interface) has previously been used in the MA calculations for thin films and multilayers.<sup>32–37</sup> It has been shown that such approximate CFS have a large effect on the MA energies.<sup>32,33</sup>

In the present paper, we calculate  $V_{i\mu\nu}^{\text{CFS}}$  for  $d$  orbitals  $\mu$ ,  $\nu$  centered on an atom  $i$  as the sum<sup>51</sup>

$$V_{i\mu\nu}^{\text{CFS}} = \sum_j v_{i\mu\nu;j}^{\text{CFS}} \quad (9)$$

over its first nearest neighbors; we neglect CFS for  $s$  and  $p$  orbitals and all  $sp$ ,  $sd$ ,  $pd$  off-diagonal terms  $V_{i\mu\nu}^{\text{CFS}}$ . In Eq. (9), the terms  $v_{i\mu\nu;j}^{\text{CFS}}$  are given by expressions formally identical<sup>50</sup> to the SK formulas where the two-center hopping integrals  $V_{dd\sigma}$ ,  $V_{dd\pi}$ ,  $V_{dd\delta}$  are replaced with similar parameters  $v_{dd\sigma}^{\text{CFS}}(m, m')$ ,  $v_{dd\pi}^{\text{CFS}}(m, m')$ ,  $v_{dd\delta}^{\text{CFS}}(m, m')$  describing CFS. These two-center CFS parameters depend on the types  $m$  and  $m'$  of the atoms  $i$  and  $j$ , correspondingly, each of which is either Co or Cu.

This method of calculating CFS in TB models has been presented in Ref. 51 and used in some theoretical papers.<sup>52–55</sup> A more general approach to the on-site energies is described in Ref. 56 while a different method using the Fourier transform of the potential is applied to find the CFS in the bulk cubic crystals in an early work on the TB model by Callaway and Edwards.<sup>57</sup> The expressions for  $V_{i\mu\nu}^{\text{CFS}}$  and  $v_{i\mu\nu;j}^{\text{CFS}}$  can be derived similarly as the SK formulas, i.e., by approximating the potential  $V^\sigma(\mathbf{r})$  with the sum of spherically symmetric atomic potentials  $v_j^\sigma(|\mathbf{r}-\mathbf{R}_j|)$  and expressing the orbitals  $\mu$  and  $\nu$  centered on atom  $i$  in terms of the orbitals with the angular momentum quantized along the axis joining the atoms  $i$  and  $j$ . Then, the on-site energies  $V_{i\mu\nu}^\sigma$  found as the matrix elements of the Hamiltonian  $-\frac{1}{2}\nabla^2 + V^\sigma(\mathbf{r})$ , include the terms  $\langle i\mu|v_j^\sigma|i\nu\rangle$  which, after neglecting their spin dependence, are denoted as  $v_{i\mu\nu;j}^{\text{CFS}}$  in Eq. (9). One concludes here that the elements  $v_{i\mu\nu;j}^{\text{CFS}}$  are, in general, *not* symmetrical in  $i$ ,  $j$ , and nor do the two-center CFS parameters, like  $v_{dd\sigma}^{\text{CFS}}(m, m')$ , need to have the same values for  $(m, m') = (\text{Co}, \text{Cu})$  and  $(m, m') = (\text{Cu}, \text{Co})$ .

Because, the term  $V_{i\mu\nu}^{\text{CFS}}$  becomes  $V_{i\mu\nu}^{\text{CFS}} + c\delta_{\mu\nu}$  under the uniform shift  $v_{dd\eta}^{\text{CFS}} \rightarrow v_{dd\eta}^{\text{CFS}} + c$  ( $\eta = \sigma, \pi, \delta$ ), we can include  $v_{dd\delta}^{\text{CFS}}$  into the diagonal on-site term  $U_{il;\sigma}$ , Eq. (8), and assume that  $v_{dd\delta}^{\text{CFS}} = 0$  hereafter. We determine the values of  $v_{dd\sigma}^{\text{CFS}}$  and  $v_{dd\pi}^{\text{CFS}}$  by fitting the energies obtained with our tight-binding model for paramagnetic Co and Cu monolayers to the *ab initio* bands.<sup>58</sup> As a result, we have found the values  $v_{dd\sigma}^{\text{CFS}}(m, m) = -0.17$  eV and  $v_{dd\pi}^{\text{CFS}}(m, m) = -0.10$  eV, valid for both  $m = \text{Co}$  and  $m = \text{Cu}$  within the accuracy of the fitting method. The same values are assumed for the parameters  $v_{dd\sigma}^{\text{CFS}}(m, m')$ ,  $v_{dd\pi}^{\text{CFS}}(m, m')$  used to find the contribution of a Cu atom to the on-site energy  $V_{i\mu\nu}^\sigma$  on a neighboring Co atom, i.e., for  $(m, m') = (\text{Co}, \text{Cu})$ , or vice versa, i.e., for  $(m, m') = (\text{Cu}, \text{Co})$ . Thus, we can obtain, e.g., the splitting of 0.10 eV between the on-site energies of  $zx$  and  $yz$  orbitals for atoms located on the step edge. Similarly, we find that the orbitals  $3z^2 - r^2$  and  $x^2 - y^2$  are split by 0.20 eV at the flat film surface; this value is close to the splitting of 0.22 eV between out-of-plane and in-plane orbitals assumed previously for Co slabs.<sup>33,37</sup> We do not scale the two-center CFS parameters when the interatomic distances change slightly in systems with relaxed structure; the canonical scaling law used for the hopping integrals seems not to be valid in this case.

The on-site energies of down- and up-spin  $d$  orbitals on Co atoms are split by the exchange interaction,

$$U_{il\downarrow} = U_{il}^{(0)} + \frac{1}{2}\Delta_{\text{ex}}^{(i)}, \quad (10a)$$

$$U_{il\uparrow} = U_{il}^{(0)} - \frac{1}{2}\Delta_{\text{ex}}^{(i)} \quad (10b)$$

( $l=2$ ). The exchange splitting

$$\Delta_{\text{ex}}^{(i)} = \Delta_{\text{ex}}^{\text{bulk}} \frac{M_i}{M_{\text{bulk}}} \quad (11)$$

on a Co atom  $i$  is proportional to its spin moment  $M_i$ . Here, we assume that the exchange splitting in bulk fcc Co is  $\Delta_{\text{ex}}^{\text{bulk}} = 1.8$  eV (cf. Ref. 59) which, in the present TB model, leads to the bulk spin magnetic moment  $M_{\text{bulk}} = 1.57\mu_B$ , close to the *ab initio* values.<sup>60,61</sup> No exchange splitting is assumed for  $s$  and  $p$  orbitals on Co atoms and for all orbitals on Cu atoms.

To find the yet undetermined on-site energy terms  $U_{il}^{(0)}$  we require charge neutrality, assumed separately for the  $d$  orbitals,

$$n_d^{(i)} = n_d^{\text{bulk};m}, \quad (12)$$

and the  $s$  and  $p$  orbitals,<sup>62</sup>

$$n_{sp}^{(i)} = n_s^{(i)} + n_p^{(i)} = n_s^{\text{bulk};m} + n_p^{\text{bulk};m}. \quad (13)$$

The quantities  $n_s^{(i)}$ ,  $n_p^{(i)}$ , and  $n_d^{(i)}$  are the projected  $s$ ,  $p$ , and  $d$  occupations on an atom  $i$  while  $n_s^{\text{bulk};m}$ ,  $n_p^{\text{bulk};m}$ , and  $n_d^{\text{bulk};m}$  are the corresponding values found with the present TB model for the respective bulk metal  $m$ : ferromagnetic fcc Co or paramagnetic Cu. The conditions (12) and (13) are well satisfied at transition-metal surfaces as found in the *ab initio* calculations<sup>61</sup> and have been used previously in TB models (cf., e.g., Refs. 31, 37, and 63).

According to Eqs. (12) and (13), we usually assume that there is *no* CT in the investigated systems. However, for selected decorated Co( $N/N-1$ ) steps, we study the effect of CT between Cu and Co atoms which leads to nonzero charges  $-q_i|e|$  on atoms  $i$  around the step edge. For this purpose, it is assumed here that a Co atom acquires  $q_{\text{tr}}$  electrons from *each* of its first-nearest Cu neighbors so that  $-q_{\text{tr}}|e|$  is the charge transferred per one Cu-Co bond. In consequence, the corresponding electron occupations  $n_d^{(i)}$  and  $n_{sp}^{(i)}$ , originally given by the right-hand sides of Eqs. (12) and (13), must be modified slightly. So, we assume that only the  $d$ -orbital occupation  $n_d^{(i)}$  changes, by the amount  $q_i > 0$ , on Co atoms, due to a relatively large value of the local  $d$ -orbital-projected density of states (DOS) at the Fermi level. Further, it is assumed that the changes of the occupations  $n_d^{(i)}$  and  $n_{sp}^{(i)}$  on Cu atoms are equal,  $\Delta n_d^{(i)} = \Delta n_{sp}^{(i)} = q_i/2$ . It should be noted here that the actual distribution between the  $sp$  and  $d$  orbitals of the electron deficiency  $q_i = -5q_{\text{tr}}$  on the decorating Cu atoms is found to be irrelevant as far as UIP-MA is concerned. The approximate value  $q_{\text{tr}} = 0.025$  is obtained by fitting, within the applied TB model, the decrease  $M_i - M_{\text{bulk}}$  of the Co magnetic moment  $M_i$  at the Co/Cu interface in the (001) fcc Co(6)/Cu(10) slabs to the *ab initio* value  $M_i - M_{\text{bulk}} = -0.06\mu_B$  found in Ref. 64.

### C. Calculation methods: on-site energies, magnetocrystalline anisotropy

The orbital-projected occupations  $n_s^{(i)}$ ,  $n_p^{(i)}$ ,  $n_d^{(i)}$ , as well as the atomic moments  $M_i$ , can be obtained easily once the diagonal part of the system's Green function (GF)  $G(z) = (z - H_{\text{TB}})^{-1}$  is known.<sup>34,65</sup> We determine the GF elements  $\langle i\mu\sigma | G(z) | i\mu\sigma \rangle$  for a number of atoms  $i$  around the step by using the recursion method (RM).<sup>65</sup> We do this for all atomic wires which are distant by less than 1.5 lattice constants ( $a_0$ ) in the  $x$  (i.e.,  $[1\bar{1}0]$ ) direction from the step edge; in each wire, we choose one atom with the smallest  $y$   $[=0$  or  $a_0/(2\sqrt{2})]$  coordinate. The on-site energy terms  $U_{il}^{(0)}$  are then found for the chosen atoms by solving Eqs. (12) and (13) (appropriately modified for  $q_{\text{tr}} \neq 0$ ) iteratively. For every iteration, the new value of  $U_{i2}^{(0)}$  for an atom  $i$  (as well as for all other, equivalent, atoms belonging to the same wire as the atom  $i$ ) is expressed only with the values of  $U_{i2}^{(0)}$  and  $n_d^{(i)}$  found in previous iteration steps. This means that, for each atom  $i$ , Eq. (12) is solved as if it were a nonlinear equation for a single variable  $U_{i2}^{(0)}$ . Similar assumption is made for Eq. (13) and its dependence on  $U_{i0}^{(0)}$  and  $U_{i1}^{(0)}$ .<sup>66</sup> Despite such approximate way of solving the multiatom set of Eqs. (12) and (13), which are obviously interdependent to some extent, only around 15 iterations are usually needed to fulfill Eqs. (12) and (13) for all atoms  $i$  with the absolute error less than 0.0001. A similar technique was previously successful for determination of layer on-site energies in thin magnetic films and multilayers.<sup>33,37</sup> The success of such algorithm proves *a posteriori* that the occupation  $n_d^{(i)}$  on an atom  $i$  depends mainly on the term  $U_{i2}^{(0)}$  (i.e., for  $l=2$ ) determining the on-site energies of  $d$  orbitals on the same atom  $i$ ; similarly,  $n_s^{(i)} + n_p^{(i)}$  depends mainly on  $U_{i0}^{(0)}$  and  $U_{i1}^{(0)}$  ( $l=0,1$ ).

The occupations  $n_s^{(i)}$ ,  $n_p^{(i)}$ ,  $n_d^{(i)}$  and the moments  $M_i$  for atoms  $i$ , which lie farther than  $1.5a_0$  from the step edge, are to a good approximation not affected by its presence. Therefore, the on-site energy terms  $U_{il}^{(0)}$  for these atoms are the same as for flat slabs,<sup>37</sup>  $N$  or  $N-1$  monolayers thick, and they are determined separately, prior to the main calculation for the Co( $N/N-1$ ) step.

The magnetocrystalline contribution to the UIP-MA constant  $K_u$ , Eq. (2), is calculated with use of the force theorem,<sup>67,68</sup>

$$K_u^{\text{MCA}} = \Omega\left(\theta, \phi = \frac{\pi}{2}\right) - \Omega(\theta, \phi = 0) \quad \left(\theta = \frac{\pi}{2}\right). \quad (14)$$

The electronic grand thermodynamic potential for a given magnetization direction  $(\theta, \phi)$ ,

$$\Omega(\theta, \phi) = -k_B T \int dE \ln \left( 1 + \exp \frac{\epsilon_F - E}{k_B T} \right) n(E), \quad (15)$$

is expressed in terms of the GF via the total density of states (DOS)

$$n(E) = -\frac{1}{\pi} \text{Im Tr } G(E + i\delta) \quad (16)$$

( $\delta \rightarrow 0+$ );  $\epsilon_F$  is the Fermi energy and  $k_B$  is the Boltzmann constant [in Eqs. (16) and (17) exclusively,  $i$  denotes  $\sqrt{-1}$ ]. We use thermodynamic potential  $\Omega$  for a finite temperature  $T$  ( $=300$  K) instead of zero-temperature energy  $E$  because such approach has previously been found to help MA energies converge for flat thin films due to the thermal smearing of the Fermi level.<sup>34,37</sup> However, it should be stressed that finite  $T$  is used *only* as a convenient tool in the numerical calculations. In particular, the present model does not account for the decrease of the spontaneous magnetization which occurs in real systems at finite temperatures due to magnetic excitations (cf. Refs. 34 and 37).

We calculate the GF and hence the uniaxial in-plane magnetocrystalline anisotropy (UIP-MCA) constant using two distinct methods. The first one applies the standard RM to find the diagonal GF elements entering the expression for the DOS,

$$n(E) = -\frac{1}{\pi} \sum_{j\kappa} \text{Im} \langle j\kappa | G(E + i\delta) | j\kappa \rangle, \quad (17)$$

which comes from the general formula (16) when the trace is calculated with the states

$$|j\kappa\rangle = \frac{1}{\sqrt{2}} (|j\mu\uparrow\rangle \pm |j\mu\downarrow\rangle). \quad (18)$$

These states are chosen instead of the states  $|j\mu\uparrow\rangle$ ,  $(|j\mu\downarrow\rangle)$ , because the continued fractions that express the diagonal GF elements in the RM converge much quicker in this case (cf. Ref. 69). However, still as many as 400 levels of the continued fraction for  $d$  orbitals and 120 for  $s$  and  $p$  ones are required to calculate  $K_u^{\text{MCA}}$  with the accuracy of 0.01 meV/(step atom) (i.e., per one atom on the step edge);<sup>70</sup> similar number of levels have been applied in Ref. 71.

The UIP-MCA constant determined with RM is given by the sum of the atomic contributions

$$K_u^{\text{MCA}} = \sum_j k_{u,\text{MCA}}^{(j)}. \quad (19)$$

To reach the accuracy 0.01 meV/(step atom) for  $K_u^{\text{MCA}}$ , it is sufficient to include the contributions  $k_{u,\text{MCA}}^{(j)}$  from all atomic wires which are within the  $3.5a_0$  distance from the step edge (cf. Figs. 5–7 and the discussion below); again we choose one atom with the smallest  $y$  coordinate in each atomic wire.

A many-fold reduction of the computational cost in the RM calculations of  $K_u^{\text{MCA}}$ , as well as  $n_s^{(i)}$ ,  $n_p^{(i)}$ ,  $n_d^{(i)}$  is obtained by truncating the Co( $N-1/N$ ) step, nominally infinite in-plane, to a finite cluster with the square base which is centered at  $x=y=0$  and has its two sides parallel to the step edge. It has been found that the effect of the introduced cluster boundaries is so small that  $K_u^{\text{MCA}}$  does not change by more than 0.01 meV/(step atom) provided that the cluster size in the  $x$  and  $y$  directions exceeds  $50a_0$ . This theoretical finding is interesting because the coefficients in the continued fraction are obtained through iterative application of the

TB Hamiltonian  $H_{\text{TB}}$ , Eq. (6), on an initial state, like  $|j\kappa\rangle$ , located on an atom close to the cluster center. Thus, these coefficients start to be disturbed by the presence of the boundaries already after around 25 iterations for the assumed cluster size. Similarly, a cluster length and width of more than  $30a_0$  guarantees that the errors in the occupations  $n_s^{(i)}$ ,  $n_p^{(i)}$ ,  $n_d^{(i)}$  and the moments  $M_i$  are less than 0.0001 for atoms lying close to the cluster center. This being true despite the fact that the number of levels in the continued fraction required for such high accuracy is 30 for  $s$  and  $p$  orbitals, and 120 for  $d$  ones.

Because, a few hundred levels of the continued fraction are needed to obtain well-converged results for the UIP-MCA constant, this calculation becomes difficult for  $\text{Co}(N/N-1)$  steps with thicknesses  $N$  larger than 6 ML due to the long computation times required. To remedy this situation, a new method, based on the Mobius transformation (MT) approach<sup>72</sup> to calculate the GF, has been developed. First, the energy  $E$  (or grand potential  $\Omega$ ) is shown to have the following general form:

$$E(\theta, \phi) = E_{\text{const}} + E_{\text{bulk}}L + E_{\text{osc}}(L), \quad (20)$$

where  $L$  is the length of the  $\text{Co}(N/N-1)$  step after truncating it only in the  $x$  direction; the truncated system remains infinite in the  $y$  direction. The MT method allows us to determine each energy term, present in Eq. (20), separately. The term  $E_{\text{osc}}(L)$ , is an oscillatory function of  $L$  and comes from the interference between the boundaries of the truncated step. This goes to 0 for the infinite step, i.e., for  $L \rightarrow \infty$ . The bulk term  $E_{\text{bulk}}(\theta, \phi)$  is the sum of the energies of the disconnected *flat* slabs,  $N$ - and  $(N-1)$ -monolayers thick, and as such it contributes only to the cubic MA constant  $K_1$  in the in-plane dependence of the step energy on the magnetization direction  $(\theta, \phi)$ , Eq. (1). The constant term  $E_{\text{const}}$  includes the contributions  $E_{\text{ends}}$  coming from the boundaries of the truncated step (which are located at  $x = -L/2$  and  $x = L/2$ ). These, unwanted contributions can be found separately (by considering truncated flat slabs), and thus eliminated from  $E_{\text{const}}$ , leaving the the contribution  $E_{\text{step}}$  coming from the step region alone,

$$E_{\text{step}} = E_{\text{const}} - E_{\text{ends}}. \quad (21)$$

Finally, the UIP-MCA constant is calculated as

$$K_u^{\text{MCA}} = E_{\text{step}}\left(\phi = \frac{\pi}{2}\right) - E_{\text{step}}(\phi = 0) \quad (22)$$

( $\theta = \frac{\pi}{2}$ ). More details of this MT approach can be found in Ref. 31 while the full description will be presented elsewhere.<sup>73</sup> The MT method is much more efficient computationally than RM and allowed us to obtain accurate values of the UIP-MCA constants for steps  $\text{Co}(N/N-1)$  with thicknesses  $N$  up to 10 ML.

### III. RESULTS: COMPARISON WITH EXPERIMENT

The atomic spin magnetic moments obtained within the described TB model by using RM are presented in Fig. 3. The moments at the Co film surface are enhanced, in com-

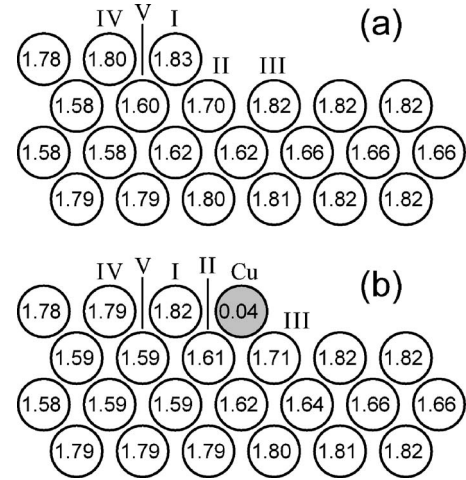


FIG. 3. Atomic magnetic moments  $M_i$  (in  $\mu_B$ ) for the (001) fcc  $\text{Co}(4/3)$  step: (a) undecorated, (b) decorated with one Cu wire. The results are obtained within the TB model including *neither* CFS *nor* structure relaxation (cf. Sec. II B). Selected Co atoms are marked with Roman numbers for reference in text.

parison to bulk, and similar results have been found in *ab initio* calculations.<sup>59,61</sup> The moment of Co atoms at the very step edge is further enhanced. This confirms the general rule that the local magnetic moment, as well as the local exchange splitting, are the larger the smaller the atom's coordination number, which is a consequence of the reduced local  $d$ -orbital-projected density of states due to the decreased hopping. A closer comparison of Figs. 3(a) and 3(b) reveals that the decorating Cu atom modifies the moments of the neighboring Co atoms, due to the Co-Cu hybridization, as if it were a Co atom; at the same time the Cu atom acquires only a very small, induced, magnetic moment. In particular, the moments of Co atoms labeled II and III in Fig. 3 become, after decoration, very close to the moments of the atoms V and II, respectively, before decoration. This resembles the situation at the interface of Co and Cu films where the Co moments are very close to the bulk Co moments.<sup>55,64</sup> Similar behavior and values of the moments around the step edge have been previously found with tight-binding linear-muffin-tin-orbital method in Ref. 28. Presently, we have also found that the inclusion of CFS, biaxial strain and local structure relaxation, discussed above, modifies magnetization very weakly: atomic moments change by no more than  $0.02\mu_B$  in comparison to those shown in Fig. 3.

Slightly larger changes of Co atomic moments are induced by the CT between Cu and Co atoms if we assume that it takes place. Indeed, we find for the decorated  $\text{Co}(4/3)$  step that the moments on Co atoms I, II, III decrease from  $1.821\mu_B$ ,  $1.599\mu_B$ ,  $1.722\mu_B$ , respectively, for  $q_{\text{tr}}=0$ , to the corresponding values  $1.794\mu_B$ ,  $1.544\mu_B$ ,  $1.668\mu_B$  found with the fitted value  $q_{\text{tr}}=0.025$  of CT per Cu-Co bond; all these moments are obtained within the TB model with CFS and structure relaxation included. The moment change  $\Delta M_i$  induced by CT is very close to the negative value of the local electron excess  $q_i$  on Co atom  $i$ , this being  $q_i=q_{\text{tr}}$  for atom I, and  $q_i=2q_{\text{tr}}$  for atoms II, III. This happens because the condition  $\Delta n_d^{(i)}=q_i$  has been assumed to hold for Co atoms, on

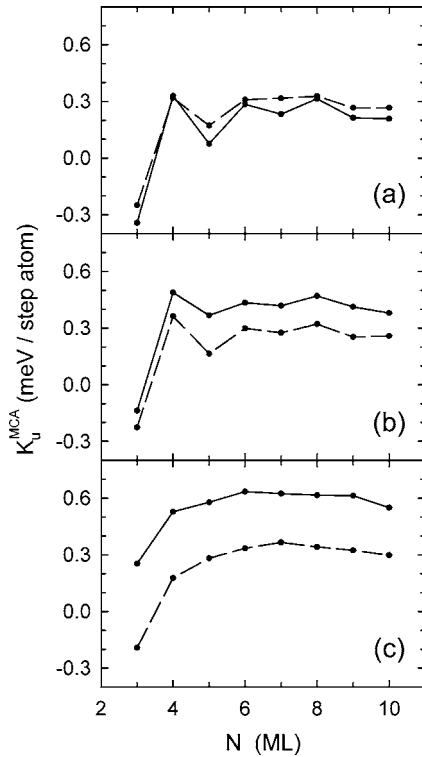


FIG. 4. UIP-MCA constant  $K_u^{\text{MCA}}$  [cf. Eq. (14)] vs Co film thickness  $N$  calculated for (001) fcc  $\text{Co}(N/N-1)$  steps: undecorated (solid line) and decorated with one Cu wire (broken line); cf. Fig. 1. The results are obtained within the TB model (cf. Sec. II B) which includes: (a) *neither* CFS *nor* structure relaxation, (b) CFS but *no* structure relaxation, (c) *both* CFS and structure relaxation.

which the minority-spin component of DOS at the Fermi level is much larger than the majority-spin one.

Because, the decoration of  $\text{Co}(N/N-1)$  step with Cu atoms modifies the Co magnetic moments only in the immediate vicinity of the Co step edge (Fig. 3), the resulting change in the dipole-dipole energy is minute.<sup>38</sup> Thus, we can neglect the dipolar contribution  $K_u^{\text{dip}}$  to the UIP-MA constant  $K_u$  in the *present* study which is focussed on the effect of the step decoration. However, in general, this contribution is not negligible: it is positive and favors a magnetization lying parallel to the step edge. The calculations of  $K_u^{\text{dip}}$  for magnetic films on vicinal surfaces and networks of magnetic stripes deposited on flat or vicinal surfaces will be presented elsewhere.<sup>38</sup>

The calculations of the UIP-MCA constant  $K_u^{\text{MCA}}$  have been done in three consecutive stages. The CFS are included in the TB model in the second stage and structure relaxations in the third, while the initial TB model, i.e., in the first stage, includes neither of the two above ingredients. However, at every stage, the on-site energy terms  $U_{ij}$  are found as described in Sec. II. All the results for  $K_u^{\text{MCA}}$  are gathered in Fig. 4. In each of the three variants of the TB model, the obtained  $K_u^{\text{MCA}}$  is positive for both decorated and undecorated  $\text{Co}(N/N-1)$  steps with thicknesses  $N \geq 4$ . When no CFS nor structure relaxation are present the step decoration with Cu has only small effect on  $K_u^{\text{MCA}}$ : it is changed by no more than 0.05 meV/(step atom) and the shift is positive.<sup>74</sup>

TABLE I. UIP-MCA constant  $K_u^{\text{MCA}}$  [in meV/(step atom)] of (001) fcc  $\text{Co}(4/3)$  and  $\text{Co}(6/5)$  steps decorated with one Cu wire. The results obtained within the TB model which includes CFS, structure relaxation, and CT of  $q_{\text{tr}}$  electrons per Cu-Co bond.

	$q_{\text{tr}}=0$	$q_{\text{tr}}=0.025$	$q_{\text{tr}}=0.05$
$\text{Co}(4/3)$	0.18	0.17	0.15
$\text{Co}(6/5)$	0.33	0.32	0.28

The presence of CFS shifts the UIP-MCA constant  $K_u^{\text{MCA}}$  of the *undecorated* steps upwards by around 0.2 meV/(step atom); the inclusion of structure relaxation results in a further, slightly smaller, shift. At the same time, the average value of  $K_u^{\text{MCA}}$  for decorated steps remains almost unchanged, being close to 0.3 meV/(step atom) for  $N \geq 6$  ML, regardless of whether the CFS or structure relaxation are included. As a net result, the decoration decreases  $K_u^{\text{MCA}}$  by 0.15–0.20 meV/(step atom) or 0.25–0.30 meV/(step atom) when only CFS or both CFS and relaxation, correspondingly, are included.

Another mechanism which, in principle, could affect the UIP-MCA constant is CT between the decorating Cu atoms and the neighboring Co atoms. To study this possibility, we have calculated the UIP-MCA constant for the decorated  $\text{Co}(4/3)$  and  $\text{Co}(6/5)$  steps using the fitted value  $q_{\text{tr}}=0.025$  and its double,  $q_{\text{tr}}=0.05$ . The results shown in Table I prove that CT has very small effect on the UIP-MCA constant for  $q_{\text{tr}}=0.025$ . For  $q_{\text{tr}}=0.05$ , the change of  $K_u^{\text{MCA}}$  is somewhat larger but it is still much smaller than the shift of  $K_u^{\text{MCA}}$  due to CFS or structure relaxation. Thus, we conclude that CT is not responsible for the UIP-MCA shift induced by the step decoration and it can be neglected in the further discussion. However, this conclusion should not be generalized to other systems where larger interatomic charge transfers can take place and lead to more significant changes of MCA energies as a result of larger shifts of the local DOS with respect to the Fermi level.

The obtained  $K_u^{\text{MCA}}$ , shown in Fig. 4, oscillates with a period close to 2 ML when the step thickness  $N$  increases. Similar 2-ML oscillations of out-of-plane MCA constant have previously been found for flat Co films<sup>37</sup> and Co/Cu multilayers.<sup>75</sup> It has been shown<sup>37</sup> that these oscillations originate from the quantum well (QW) states present in the Co layer which have  $\mathbf{k}$  vectors in the center of the two-dimensional Brillouin zone and energies close to the Fermi level. Similar QW states are likely to be responsible for the oscillations of  $K_u^{\text{MCA}}(N)$  in the  $\text{Co}(N/N-1)$  steps. Interestingly, such oscillations are absent once the atomic structure is allowed to relax [cf. Fig. 4(c)]; explanation of this behavior needs further study, especially, in connection to the absence of such oscillations in experiment.<sup>10,12</sup>

To compare the obtained results with the experimental data found for Co films on vicinal (001) Cu surfaces, we convert the measured  $H_s$  field, given in kA/m, into the UIP-MA constant  $K_u$ :

$$K_u = 1.254 \times 10^{-4} N N_{\text{rows}} H_s \quad [\text{meV}/(\text{step atom})]; \quad (23)$$

here  $N_{\text{rows}}$  is the terrace width which depends on the miscut angle  $\alpha$  through Eq. (4). In Ref. 11, the  $H_s$  field is found

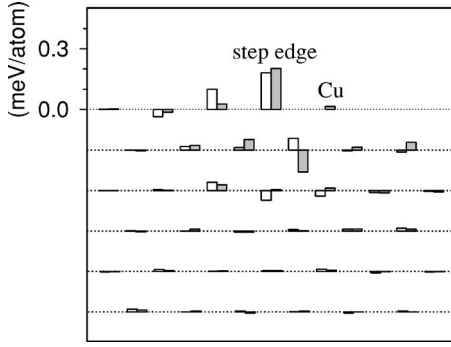


FIG. 5. Atomic contributions  $k_{u;MCA}^{(i)}$  (bars) to UIP-MCA constant  $K_u^{MCA}$  [cf. Eq. (19)] for (001) fcc Co(6/5) step: undecorated (white bars) and decorated (grey bars) with one Cu wire. The horizontal dotted lines mark (001) atomic planes; atomic wires (Co or Cu) are located at points where the bars touch the lines which also serve as the zero reference levels for the bars. The plotted data are obtained within the TB model which includes *neither* CFS *nor* structure relaxation (cf. Sec. II B).

experimentally for  $\alpha=3.4^\circ$  and the Co film thicknesses  $N=9.4, 10.8,$  and  $13.2$  ML. By taking the corresponding values,  $\Delta H_s=-13.5, -11.5,$  and  $-12.5$  kA/m, of the differences  $\Delta H_s=H_s^{\text{dec}}-H_s^{\text{undec}}$  between the minimum  $H_s$  field found for the decorated films,  $H_s^{\text{dec}}$ , and the field  $H_s^{\text{undec}}$  for the undecorated film, we obtain with Eq. (23) the respective experimental shifts  $\Delta K_u=-0.19, -0.19,$  and  $-0.25$  meV/(step atom) of the UIP-MA constant. A very similar value of  $\Delta K_u$  is found from the data reported in Ref. 13 for 8 ML Co film deposited on slightly curved Cu surface which has a variable miscut angle  $\alpha (\leq 5.4^\circ)$ . It was shown there that  $H_s$  depends linearly on  $\alpha$  and it vanishes after deposition of an amount of Cu sufficient to decorate 70% of Co steps with single Cu wires. This result allows us to write the equation

$$0.3H_s^{\text{undec}} + 0.7H_s^{\text{dec}} = 0, \quad (24)$$

from which we find that  $H_s^{\text{dec}}=-0.43H_s^{\text{undec}}$  and  $\Delta H_s=-1.43H_s^{\text{undec}}$ . Thus, from the experimental value<sup>13</sup>  $H_s^{\text{undec}} \approx 150$  Oe = 11.94 kA/m found for  $\alpha=3^\circ$ , we get  $\Delta K_u=-0.23$  meV/step atom). The experimental values of the UIP-MA shift  $\Delta K_u$  derived above are close to our theoretical results obtained both with or without the structure relaxation, provided that CFS are included. We regard the remaining discrepancy of 0.05–0.01 meV/(step atom) as very low since calculated MA energies, even those found with *ab initio* methods rarely match the experimental data perfectly. Good theoretical prediction for  $\Delta K_u$  confirms the conclusion of the experimental work reported in Ref. 13 that the decrease of  $K_u$  is caused only by the Cu adsorbates located near the step edges. However, we do not obtain the sign change of  $K_u$  after decoration which is usually observed experimentally<sup>7,9,11,13</sup> and leads to switching of the magnetization direction within the plane. Indeed, after the decoration,  $K_u^{MCA}$  remains positive (for  $N \geq 4$ ); adding the dipolar contribution  $K_u^{\text{dip}}$  will push the resulting  $K_u$  even higher. This implies that the theoretical energies  $K_u^{MCA}$  are too large in comparison with experiment, both for undecorated and decorated steps. This discrepancy is presumably due to some unaccounted terms of

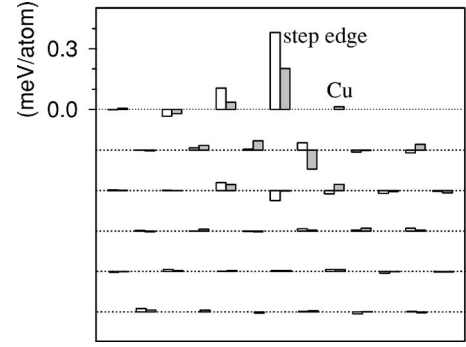


FIG. 6. Atomic UIP-MCA contributions  $k_{u;MCA}^{(i)}$  obtained for (001) fcc Co(4/3) step within the TB model which includes CFS but *no* structure relaxation (cf. Sec. II B). Other details as in Fig. 5.

volume type which are clearly present in the experimental  $H_s(N)$  dependencies.<sup>5,6</sup> The origin of such terms is not clear<sup>13,17</sup> and needs further investigation. It should be noted here that the tetragonal distortion of the biaxially strained fcc Co film lattice, which is included in our calculations, retains the films fourfold in-plane symmetry and, thus, gives no direct volume contribution to UIP-MA.<sup>13,17</sup>

To develop a better understanding the origin of the obtained shift  $\Delta K_u^{MCA}$ , we examine the contributions  $k_{u;MCA}^{(i)}$  to the UIP-MCA constant from individual atoms around the step; see Figs. 5–7. The largest contribution  $k_{u;MCA}^{(i)}$  comes from the Co atomic wire at the very step edge, marked as atom I in Fig. 3. Other atomic wires that lie within the distance  $d_w$  of  $1.5a_0$  from the step edge, give smaller, but still quite sizeable contributions  $k_{u;MCA}^{(i)}$ . The contributions from farther lying atomic wires decay very quickly with increasing  $d_w$ . However, as already mentioned above, the contributions from several tens of atomic wires with  $0 \leq d_w \leq 3.5a_0$  are required to obtain  $K_u^{MCA}$  with the accuracy of 0.01 meV/(step atom). The step decoration with Cu atoms affects UIP-MCA in three different ways. First, the additional electron hopping between the Cu atoms and the neighboring Co atoms affects contributions around the step edge, mainly on atoms II and IV, for which the respective contributions  $k_{u;MCA}^{(i)}$  are shifted downwards after decoration. However, shifts  $\Delta k_{u;MCA}^{(i)}$  of both signs are found for several atoms

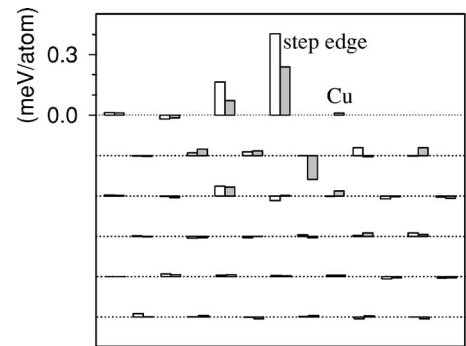


FIG. 7. Atomic UIP-MCA contributions  $k_{u;MCA}^{(i)}$  obtained for (001) fcc Co(4/3) step within the TB model which includes *both* CFS and structure relaxation (cf. Sec. II B). Other details as in Fig. 5.

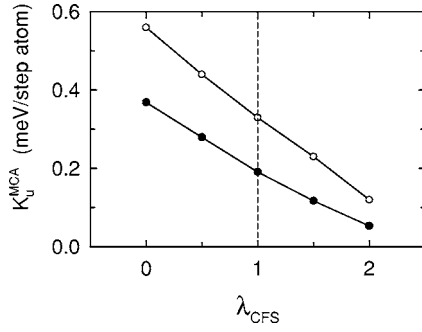


FIG. 8. UIP-MCA constant  $K_u^{\text{MCA}}$  for the (001) fcc Co(4/3) (solid circles) and Co(6/5) (open circles) steps decorated with one Cu wire; cf. Fig. 1(b). The results are plotted versus the multiplier  $\lambda_{\text{CFS}}$  that modifies the CFS contributions from the Cu atoms; cf. Eq. (25); see text. The results are obtained within the TB model including *both* CFS and structure relaxation (cf. Sec. II B). The vertical dashed line denotes the nominal value  $\lambda_{\text{CFS}}=1$ .

around the step and, thus, they tend to cancel out to a large extent which explains why the resulting total shift  $\Delta K_u^{\text{MCA}}$ , shown in Fig. 4(a), is relatively small. The inclusion of CFS leads to a large shift of  $k_{u,\text{MCA}}^{(i)}$  on the step-edge atom (atom I), for the undecorated steps, while the contributions from other atoms remain almost unchanged. This means that the UIP-MCA is affected only very locally by CFS. Indeed, the effect of CFS on atom I is canceled once the step is decorated with Cu atoms; cf. Fig. 6. This happens because the decorating Cu atoms remove, via Eq. (9), the splitting between the energies of in-plane orbitals, like  $yz$  and  $zx$ , located on atom I. On the other hand, the structural relaxation has a more spatially extended effect on UIP-MCA: it results in small changes of the contributions  $k_{u,\text{MCA}}^{(i)}$  for several atoms, both for undecorated and decorated steps. This is presumably the indirect effect of the tetragonal lattice distortion which changes the electronic structure. Furthermore, the local change of the geometric structure induced by the step decoration modifies the shifts  $\Delta k_{u,\text{MCA}}^{(i)}$  also only locally, mainly on atoms I to V around the step. In each variant of the TB model, the total UIP-MCA shift,  $\Delta K_u^{\text{MCA}}$ , can be found [with 0.01 meV/(step atom) accuracy] by adding shifts of  $k_{u,\text{MCA}}^{(i)}$  from atoms with  $0 \leq d_w \leq 2a_0$ ; cf. Ref. 31. It should also be noted that the contribution to  $K_u^{\text{MCA}}$  from the decorating Cu atom is negligible.

In order to better understand the mechanism by which CFS affect UIP-MCA, we modify the contribution of the decorating Cu atoms to CFS on the neighboring Co atoms. It is done by multiplying the CFS two-center integrals for  $m = \text{Co}$ ,  $m' = \text{Cu}$ ,

$$v_{dd\eta}^{\text{CFS}}(m, m') \rightarrow \lambda_{\text{CFS}} v_{dd\eta}^{\text{CFS}}(m, m') \quad (25)$$

with the common factor  $\lambda_{\text{CFS}}$  for  $\eta = \sigma, \pi, \delta$ ; cf. Ref. 76. In particular, for  $\lambda_{\text{CFS}}=0$ , when the Cu atoms do not contribute to CFS on the Co atoms, we find that the constant  $K_u^{\text{MCA}}$  is larger by around 0.2 meV/(step atom) than for the nominal value  $\lambda_{\text{CFS}}=1$  when the decorated steps Co(4/3) and Co(6/5) with relaxed structure are considered; cf. Figs. 8 and 4(c). In fact, the value of  $K_u^{\text{MCA}}$  for  $\lambda_{\text{CFS}}=0$  becomes

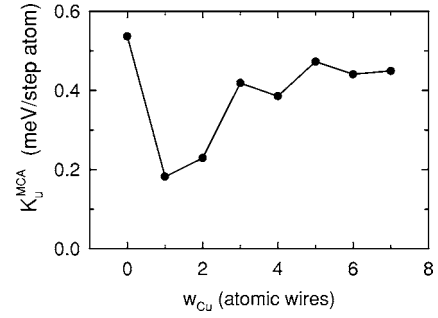


FIG. 9. UIP-MCA constant  $K_u^{\text{MCA}}$  for the (001) fcc Co(4/3) step decorated with  $w_{\text{Cu}}$  Cu wires; the data point for  $w_{\text{Cu}}=0$  corresponds to the undecorated step. The results are obtained within the TB model including *both* CFS and structure relaxation (cf. Sec. II B).

closer to  $K_u^{\text{MCA}}$  obtained for the *undecorated* step in the TB model including CFS; the remaining difference [0.08 meV/(step atom) for Co(6/5) step] is due to the change in the local structure relaxation after the step decoration. We also note that with increasing  $\lambda_{\text{CFS}}$ , the UIP-MCA constant of the decorated steps decreases, almost linearly, however, it remains positive for  $\lambda_{\text{CFS}} \leq 2$ . Thus, we do not consider possible inaccuracy in the derived two-center CFS parameters for Co and Cu as the source of the lack of magnetization switching in the present theoretical calculations.

Finally, we study how the UIP-MCA changes when more than one,  $w_{\text{Cu}}$ , Cu wires are attached to the Co step edge, in a similar way to that depicted in Fig. 1. The results obtained for  $0 \leq w_{\text{Cu}} \leq 7$  Cu wires, Fig. 9, confirm the experimental finding<sup>7</sup> that the maximum downward shift of  $K_u^{\text{MCA}}$  occurs at  $w_{\text{Cu}}=1$ . For larger  $w_{\text{Cu}}$ , the value of  $K_u^{\text{MCA}}(w_{\text{Cu}})$  increases, showing small oscillations, and saturates for  $w_{\text{Cu}} \geq 6$  at a value below, though close to, the UIP-MCA constant  $K_u^{\text{MCA}}$  for the undecorated step. A similar tendency is also observed experimentally for Cu coverage less than 1.2 ML (cf. Refs. 7 and 9) but the magnitude of experimental UIP-MA shift,  $|\Delta K_u|$ , is always larger than  $\frac{1}{2}|\Delta K_u(w_{\text{Cu}}=1)|$ .

#### IV. CONCLUSIONS

The present tight-binding calculations performed for a single step on an ultrathin (001) fcc Co slab with in-plane magnetization show that the magnetic anisotropy of vicinal Co films depends on various factors. In particular, the inclusion of crystal field splittings has been proved to be *vital* for the theoretical results to reproduce well the experimentally observed decrease of the uniaxial in-plane anisotropy energy induced by decorating the Co steps with Cu atoms. Thus, the generally assumed explanation that the shift of the uniaxial anisotropy energy is due to the local hybridization between the Co and Cu atoms, is confirmed. However, this happens *not* through the extra available hopping between Co and Cu atoms, but rather because the potential coming from the decorating Cu atoms *removes* the splitting which exists between the on-site energies of  $d$  orbitals, with different in-plane orientation, on Co atoms at the edge of the undecorated step. The fact that the crystal field splittings affect mainly the anisotropy contribution on the Co step-edge atom points to

the important role of horizontal, in-plane, bonds. Similar conclusion has previously been drawn from the experimental results through a general analysis based on the Néel's pair-bonding model.<sup>13</sup>

The investigated shift of the uniaxial anisotropy includes also a significant contribution from the local relaxation of atomic structure around the step. This finding is in agreement with the results of earlier studies (cf., e.g., Ref. 77) where strain and structure relaxation in the *flat* films have been shown to have great impact on magnetic anisotropy.

These conclusions remain valid also if the charge transfer between Cu and Co atoms around the step edge is present

since its effect on the uniaxial anisotropy energy of the vicinal Co films has been shown to be very weak.

#### ACKNOWLEDGMENTS

The authors would like to acknowledge gratefully discussions with D.M. Edwards. This work has been supported financially by the State Committee of Scientific Research (Poland) under the research project No. 2P03B 032 22 in the years 2002–2005.

\*Electronic address: mcinal@ichf.edu.pl

†Electronic address: a.umerski@open.ac.uk

- <sup>1</sup>C. Chappert, K. L. Dang, P. Beauvillain, H. Hurdequint, and D. Renard, *Phys. Rev. B* **34**, 3192 (1986).
- <sup>2</sup>M. T. Johnson, J. J. de Vries, N. W. E. McGee, J. aan de Stegge, and F. J. A. den Broeder, *Phys. Rev. Lett.* **69**, 3575 (1992).
- <sup>3</sup>P. Krams, F. Lauks, R. L. Stamps, B. Hillebrands, and G. Güntherodt, *Phys. Rev. Lett.* **69**, 3674 (1992).
- <sup>4</sup>P. Krams, B. Hillebrands, G. Güntherodt, and H. P. Oepen, *Phys. Rev. B* **49**, R3633 (1994).
- <sup>5</sup>W. Weber, R. Allenspach, and A. Bischof, *Appl. Phys. Lett.* **70**, 520 (1997).
- <sup>6</sup>C. H. Back, W. Weber, C. Würsch, A. Bischof, D. Pescia, and R. Allenspach, *J. Appl. Phys.* **81**, 5054 (1997).
- <sup>7</sup>W. Weber, C. H. Back, A. Bischof, D. Pescia, and R. Allenspach, *Nature (London)* **374**, 788 (1995).
- <sup>8</sup>Ch. Würsch, C. Stamm, S. Egger, D. Pescia, W. Baltensperger, and J. S. Helman, *Nature (London)* **389**, 937 (1997).
- <sup>9</sup>W. Weber, C. H. Back, U. Ramsperger, A. Vaterlaus, and R. Allenspach, *Phys. Rev. B* **52**, R14 400 (1995).
- <sup>10</sup>W. Weber, C. H. Back, A. Bischof, Ch. Würsch, and R. Allenspach, *Phys. Rev. Lett.* **76**, 1940 (1996).
- <sup>11</sup>W. Weber, A. Bischof, R. Allenspach, Ch. Würsch, C. H. Back, and D. Pescia, *Phys. Rev. Lett.* **76**, 3424 (1996).
- <sup>12</sup>W. Weber, A. Bischof, R. Allenspach, C. H. Back, J. Fassbender, U. May, B. Schirmer, R. M. Jungblut, G. Güntherodt, and B. Hillebrands, *Phys. Rev. B* **54**, 4075 (1996).
- <sup>13</sup>R. K. Kawakami, M. O. Bowen, H. J. Choi, E. J. Escorcia-Aparicio, and Z. Q. Qiu, *Phys. Rev. B* **58**, R5924 (1998); **60**, 713(E) (1999); *J. Appl. Phys.* **85**, 4955 (1999).
- <sup>14</sup>R. K. Kawakami, E. J. Escorcia-Aparicio, and Z. Q. Qiu, *Phys. Rev. Lett.* **77**, 2570 (1996).
- <sup>15</sup>H. J. Choi, Z. Q. Qiu, J. Pearson, J. S. Jiang, D. Li, and S. D. Bader, *Phys. Rev. B* **57**, R12713 (1998).
- <sup>16</sup>E. J. Escorcia-Aparicio, H. J. Choi, W. L. Ling, R. K. Kawakami, and Z. Q. Qiu, *Phys. Rev. Lett.* **81**, 2144 (1998).
- <sup>17</sup>H. J. Choi, R. K. Kawakami, E. J. Escorcia-Aparicio, Z. Q. Qiu, J. Pearson, J. S. Jiang, D. Li, R. Osgood, and S. D. Bader, *J. Appl. Phys.* **85**, 4958 (1999).
- <sup>18</sup>Y. Z. Wu, C. Won, and Z. Q. Qiu, *Phys. Rev. B* **65**, 184419 (2002).
- <sup>19</sup>M. Rickart, S. O. Demokritov, and B. Hillebrands, *J. Phys.: Condens. Matter* **14**, 8947 (2002).

- <sup>20</sup>M. Rickart, T. Mewes, M. Scheib, S. O. Demokritov, and B. Hillebrands, *J. Phys. D* **38**, 1047 (2005).
- <sup>21</sup>U. Bovensiepen, H. J. Choi, and Z. Q. Qiu, *Phys. Rev. B* **61**, 3235 (2000).
- <sup>22</sup>A (110) surface of a fcc crystal can be regarded as a vicinal surface with the steepest miscut angle possible ( $\alpha=45^\circ$ ) and the terrace width of just one atom.
- <sup>23</sup>J. A. C. Bland, S. Hope, B. Choi, and P. Bode, *J. Appl. Phys.* **85**, 4613 (1999).
- <sup>24</sup>W. L. Ling, Z. Q. Qiu, O. Takeuchi, D. F. Ogletree, and M. Salmeron, *Phys. Rev. B* **63**, 024408 (2000).
- <sup>25</sup>S. van Dijken, G. Di Santo, and B. Poelsema, *Phys. Rev. B* **63**, 104431 (2001).
- <sup>26</sup>The value of  $K_u$  calculated with Eq. (3) is given per unit volume of the ferromagnetic film.
- <sup>27</sup>R. Allenspach, A. Bischof, and U. Dürig, *Surf. Sci. Lett.* **381**, L573 (1997).
- <sup>28</sup>A. V. Smirnov and A. M. Bratkovsky, *Phys. Rev. B* **54**, R17371 (1996); **55**, 14434 (1997).
- <sup>29</sup>L. P. Zhong, X. D. Wang, and A. J. Freeman, *IEEE Trans. Magn.* **34**, 1213 (1998).
- <sup>30</sup>R. Gómez-Abal and A. M. Llois *Phys. Rev. B* **65**, 155426 (2002).
- <sup>31</sup>M. Cinal, A. Umerski, D. M. Edwards, and J. Inoue, *Surf. Sci.* **493**, 744 (2001).
- <sup>32</sup>P. Bruno, *Phys. Rev. B* **39**, R865 (1989).
- <sup>33</sup>M. Cinal, D. M. Edwards, and J. Mathon, *Phys. Rev. B* **50**, 3754 (1994); *J. Magn. Magn. Mater.* **140-144**, 681 (1995).
- <sup>34</sup>M. Cinal and D. M. Edwards, *Phys. Rev. B* **55**, 3636 (1997).
- <sup>35</sup>M. Cinal and D. M. Edwards, *Phys. Rev. B* **57**, 100 (1998).
- <sup>36</sup>M. Cinal, *J. Phys.: Condens. Matter* **13**, 901 (2001).
- <sup>37</sup>M. Cinal, *J. Phys.: Condens. Matter* **15**, 29 (2003).
- <sup>38</sup>M. Cinal and M. Pietrachowicz (unpublished).
- <sup>39</sup>N. A. Levanov, V. S. Stepanyuk, W. Hergert, D. I. Bazhanov, P. H. Dederichs, A. A. Katsnelson, and C. Massobrio, *Phys. Rev. B* **61**, 2230 (2000).
- <sup>40</sup>V. S. Stepanyuk, D. I. Bazhanov, A. N. Baranov, W. Hergert, P. H. Dederichs, and J. Kirschner, *Phys. Rev. B* **62**, 15398 (2000); V. S. Stepanyuk, D. I. Bazhanov, W. Hergert, and J. Kirschner, *ibid.* **63**, 153406 (2001).
- <sup>41</sup>E. Abate and M. Asdente, *Phys. Rev.* **140**, A1303 (1965).
- <sup>42</sup>A. R. Mackintosh and O. K. Andersen, in *Electrons at the Fermi surface*, edited by M. Springford (Cambridge University Press, Cambridge, 1980).

- <sup>43</sup>R. Lorenz and J. Hafner, Phys. Rev. B **54**, 15937 (1996).
- <sup>44</sup>These values have been derived for  $d$  orbitals, however no separate values are sought for  $p$  orbitals as the SO interaction between  $p$  orbitals has been found to have negligible effect on MA; cf. Ref. 33. This happens because both the exchange splitting and the orbital-projected density of states are much smaller for  $p$  orbitals than for  $d$  ones. Also, note that the SO interaction vanishes for  $s$  states.
- <sup>45</sup>J. C. Slater and G. F. Koster, Phys. Rev. **94**, 1498 (1954).
- <sup>46</sup>D. A. Papaconstantopoulos, *Handbook of the Band Structure of Elemental Solids* (Plenum, New York, 1986).
- <sup>47</sup>D. G. Pettifor, J. Phys. F: Met. Phys. **7**, 613 (1977).
- <sup>48</sup>J. Dorantes-Dávila and G. M. Pastor, Phys. Rev. Lett. **77**, 4450 (1996); **81**, 208 (1998).
- <sup>49</sup>J. M. Galagher and R. Haydock, Philos. Mag. B **38**, 155 (1978).
- <sup>50</sup>In general, when orbitals  $\mu$  and  $\nu$  have different orbital quantum numbers  $l$ , and  $l'$ , correspondingly, the expressions for  $v_{i\mu\nu j}^{\text{CFS}}$  have an extra factor  $(-1)^{(l+l')}$ , in comparison with the SK formulas.
- <sup>51</sup>D. J. Chadi, in *Atomistic Simulation of Materials: Beyond Pair Potentials*, edited by V. Vitek and D. J. Srolovitz (Plenum, New York, 1989), pp. 309–315).
- <sup>52</sup>J. L. Mercer Jr. and M. Y. Chou, Phys. Rev. B **49**, R8506 (1994).
- <sup>53</sup>R. E. Cohen, L. Stixrude, and E. Wasserman Phys. Rev. B **56**, 8575 (1997).
- <sup>54</sup>Y. Xie and J. A. Blackman, Phys. Rev. B **64**, 195115 (2001).
- <sup>55</sup>Y. Xie and J. A. Blackman, Phys. Rev. B **66**, 155417 (2002).
- <sup>56</sup>M. D. Stiles, Phys. Rev. B **55**, 4168 (1997).
- <sup>57</sup>J. Callaway and D. M. Edwards, Phys. Rev. **118**, 923 (1960).
- <sup>58</sup>E. Wimmer, J. Phys. F: Met. Phys. **14**, 2613 (1984).
- <sup>59</sup>Chun Li and A. J. Freeman, J. Magn. Magn. Mater. **75**, 53 (1988).
- <sup>60</sup>B. I. Min, T. Oguchi, and A. J. Freeman, Phys. Rev. B **33**, R7852 (1986).
- <sup>61</sup>M. Aldén, S. Mirbt, H. L. Skriver, N. M. Rosengaard, and B. Johansson, Phys. Rev. B **46**, 6303 (1992).
- <sup>62</sup>The on-site energies of  $s$ , and  $p$ , orbitals are subject to a common shift whose magnitude is chosen to satisfy Eq. (13).
- <sup>63</sup>J. Tersoff and L. M. Falicov, Phys. Rev. B **26**, 6186 (1982).
- <sup>64</sup>A. M. N. Niklasson, B. Johansson, and H. L. Skriver, Phys. Rev. B **59**, 6373 (1999).
- <sup>65</sup>R. Haydock, Solid State Phys. **35**, 215 (1980).
- <sup>66</sup>In this case, the left-hand side of Eq. (13) is treated to be the function of a common shift applied to  $U_{i0}^{(0)}$ ,  $U_{i1}^{(0)}$ .
- <sup>67</sup>L. Szunyogh, B. Újfalussy, P. Weinberger, and C. Sommers, Phys. Rev. B **54**, 6430 (1996).
- <sup>68</sup>G. H. O. Daalderop, P. J. Kelly, and M. F. H. Schuurmans, Phys. Rev. B **41**, 11919 (1990).
- <sup>69</sup>S. Pick, J. Dorantes-Dávila G. M. Pastor, and H. Dreysee, Phys. Rev. B **50**, 993 (1994).
- <sup>70</sup>We have also found that a smaller number of CF levels is needed for  $d$  orbitals when the  $spd$  hybridization is neglected.
- <sup>71</sup>S. Pick, V. S. Stepanyuk, A. N. Baranov, W. Hergert, and P. Bruno, Phys. Rev. B **68**, 104410 (2003).
- <sup>72</sup>A. Umerski, Phys. Rev. B **55**, 5266 (1997).
- <sup>73</sup>A. Umerski (unpublished).
- <sup>74</sup>In Ref. 31, the small *negative* change  $\Delta K_u^{\text{MCA}}$ , of 0.05 meV/(step atom), has been found for Co(5/4) step. However, the TB model applied there used too low values for  $M_{\text{bulk}}=1.50\mu_B$ , and the exchange splitting  $\Delta_{\text{ex}}^{\text{bulk}}=1.5$  eV.
- <sup>75</sup>L. Szunyogh, B. Újfalussy, C. Blaas, U. Pustogowa, C. Sommers, and P. Weinberger, Phys. Rev. B **56**, 14036 (1997).
- <sup>76</sup>Note that with  $v_{dd\delta}^{\text{CFS}}(m, m')=0$  it is  $v_{dd\eta}^{\text{CFS}}(m, m')-v_{dd\delta}^{\text{CFS}}(m, m')$  ( $\eta = \sigma, \pi$ ) that are really scaled.
- <sup>77</sup>O. Hjortstam, K. Baberschke, J. M. Wills, B. Johansson, and O. Eriksson, Phys. Rev. B **55**, 15026 (1997).